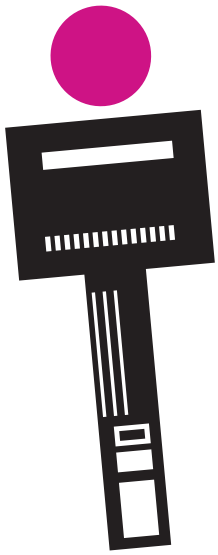

RAM ROBOTICS AND MECHATRONICS

THE VALIDATION OF A CONDUCTION MODEL OF A 3D-PRINTED OBJECT

J.E. (Justin) Vleugel

BSC ASSIGNMENT

Committee:
prof. dr. ir. G.J.M. Krijnen
ir. A.P. Dijkshoorn
dr. ir. M.P. de Jong

September, 2023

049RaM2023
Robotics and Mechatronics
EEMCS
University of Twente
P.O. Box 217
7500 AE Enschede
The Netherlands

UNIVERSITY OF TWENTE. | TECHMED CENTRE UNIVERSITY OF TWENTE. | DIGITAL SOCIETY INSTITUTE

Abstract

This study aims to investigate the validity of a model of 3D-printed conductive samples. In order to achieve this, the voltage distribution over the surfaces of real life 3D-printed samples are compared to similar modeled samples. These samples are fabricated through FDM (Fused Deposition Modeling), one of the most common forms of 3D printing. The model specifically models anisotropic behaviour in cubic samples, which means an inhomogeneous voltage distribution. In previous research performed on 2D samples, this behaviour was observed and affected by model parameters. In this paper the extent of anisotropy in 3D samples is investigated.

To attempt to affect the anisotropy in printed samples, the printing parameters and geometries of the samples are varied. These parameters include the printing temperature and the layer thickness. The samples are placed under an imposed potential difference, and the voltages on the surfaces measured using a specifically designed setup. Additional measurements are also performed to measure the resistance of the sample and verify the method. The results obtained showed little variation in anisotropy across the various samples, with all the samples being fairly isotropic. A difference in printing temperature yielded some interesting results, but more experiments must be performed to improve their reliability.

Contents

1 Introduction

Additive manufacturing, or 3D printing, is a technology that emerged in the 1980s [1], and it is used for the quick and cost-effective production of 3D objects. The objects are printed from the bottom up, without the need for any machining, straight from a computer-aided design (CAD) file [2]. There are a variety of methods for printing objects, but one of the most commonly used is fused deposition modeling (FDM). In this method, a thin layer of molten material is extruded in 'traxels', short for track-elements, or lines, which solidify after deposition. The object then consists of layers upon layers of these traxels [3]. Initially this method of 3D printing was useful mainly for printing objects for a mechanical purpose, but an emerging area of research is printing with conductive materials, of which the products are useable in electronics [4].

1.1 Conductive Prints

Printing with conductive materials has applications mainly in the realm of sensors and printed electronics. The biggest advantage of it is that sensors can be directly embedded within mechanical structures in only one manufacturing step [4]. A concrete example is the Robird, which is a robotic bird that is being developed to be used as, among other applications, a bird-control method at airports [5]. The use of sensors in this bird that are created through additive manufacturing would help to increase the functionality and adaptability of the wings in changing circumstances.

A caveat of the FDM method is that anisotropy occurs within the printed object [4].The conditions during printing can affect the quality of the bonds between adjacent traxels, affecting its electrical properties [6]. Specifically, the contact resistances between the traxels and the layers give rise to anisotropic electrical properties of the object as a whole. This is not necessarily a disadvantage, as knowledge of how specific aspects of the printing process affect the properties of the object are useful in engineering an appropriate sensor. These aspects include the width, length and height of the traxels, as well as the number [7].

1.2 Modelling the Behavior

There are multiple ways to represent the behavior of the printed objects, one of which is using FEM tools such as COMSOL. This method can be useful, but studying a large number of iterations can be time comsuming. Additionally, the underlying behavior of the system is not well-represented. An analytical model would be a more optimal solution, and this was created for 2D stratified structures by G. Krijnen and A. Dijkshoorn [8]. and later extended to 3D by D. Wilmes [7]. The principle of the model is using coupled differential equations to model potential and current distributions for each of the traxels in interaction with its adjacent traxels. The assumption is that each traxel has basic electrical properties in their own longitudinal direction and in the contacts between them. As such, the model is a system of coupled ordinary differential equations, with each equation describing the voltage and current on its respective traxel.

1.3 Goals

The goal of this paper is to validate the 3D analytical model created by Wilmes through experimental means. This means investigating whether the assumptions made by the model are compatible with the real world results. The primary method of doing so will be to use probes to directly measure current, voltage, and impedance. To achieve this, a probe station is constructed to efficiently measure a number of iterations. Various geometries will be simulated and printed, and the results then compared to the results obtained from the model.

1.4 Research Questions

In order to achieve the goal illustrated above, some specific research questions must be formulated. The main question, which asks the overarching question of this paper, is the following:

To what extent can the model be used to approximate the anisotropy of real printed samples?

To answer this question, samples with various levels of anisotropy should be produced and tested. Thus, the following question applies:

How do print settings such as nozzle temperature and layer thickness affect the anisotropy of the samples?

In order to be able to test these samples, a suitable set-up must be designed. Therefore, the following question is also relevant:

How can a set-up be designed that is capable of producing data that is comparable to the model?

1.5 Report Structure

The report is structured into seven chapters, including this introduction. Chapter 2 discusses previous research that is relevant for 3D-printing and anisotropy in 3D-printed samples. Chapter 3 discusses the workings of the model and show examples of its implementation. Chapter 4 shows the process of fabricating the samples and the various elements of the set-up. Next, chapter 5 describes the experimental set-ups and processes. The following chapter 6 presents and provides some analysis on the results obtained from experiments. Finally, chapter 7 discusses the experiments and its results, and makes conclusions based on the data obtained.

2 Background

This chapter mainly serves to introduce the research question: **How do print settings such as nozzle temperature and layer thickness affect the anisotropy of the samples?** In order to do so, previous research will be examined in order to determine if it applies to the specifics of this paper.

2.1 3D-Printing

There are a multitude of methods used in additive manufacturing. One that has been widely adopted is the fused deposition modeling (FDM) method. In this method, a filament, in extruded in adjacent traxels, layer by layer. The filament is often made of polylactic acid(PLA) or acrylonitrile butadiene (ABS) based materials. The result is a 3D structure [9].

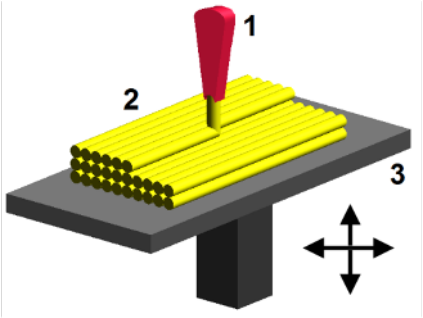

Figure 2.1: A Simplified representation of additive manufacturing [10]

A more recent development in 3D-printing is using conductive materials as filament. This would allow objects with electrical applications such as sensors to be manufactured in a single print. [2] The material used as filament in that case is a composite material of thermoplastic doped with carbon or metal. For this research, "Proto-Pasta" will be used, which is PLA with carbon black nano-particles mixed into it.

2.2 Anisotropy in 3D-Printed Objects

Anisotropy is defined as the property that different (physical) properties are measured depending on the direction in which the measurements are taken.

In general, multiple (physical) properties can show anisotropy. For this research important anisotropic properties are, resulting from FDM 3D-printing are; electrical, mechanical, and thermal. All three do occur, but the focus of this paper is conductive anisotropy. In that case, the conductivity of the structure varies along different directions [1]. The two main factors which cause this anisotropy, are the insufficient bonding between the layers, and air voids which form between adjacent traxels when printing. [1] During the printing process, the filament is heated in the heating chamber, and then rapidly cools after extrusion through the nozzle. This quick cooling can cause adjacent traxels to have bonds which vary in strength throughout the final product. This then causes mechanical and electrical anisotropy in the object. At the same time, the somewhat elliptical nature of the traxels causes air gaps in between them. These gaps are also inhomogeneous throughout the structure, possibly causing further anisotropy.

2.3 Affecting the Anisotropy

In order to validate the model the level of anisotropy will need to be varied in the physical prints. A way of representing the anisotropy quantitatively is through the anisotropy ratio. It represents the ratio between the bulk resistance of a sample, and the sum of the bulk resis-

tance and the contact resistance between adjacent traxels. Its value is between 0 and 1, with 1 representing an isotropic sample, and 0 a highly anisotropic one. This ratio can be defined as follows:

$$\Gamma_y = \frac{\rho}{\rho + \sigma_y / W} \tag{2.1}$$

$$\Gamma_z = \frac{\rho}{\rho + \sigma_z / H} \tag{2.2}$$

Where ρ is the bulk resistivity of the object, σ is the contact resistivity between the traxels, and W is the width of the traxel. This ratio can be defined both in the y- and z- directions, as the traxels in a sample have adjacent traxels in these two directions and the x-direction is chosen along the traxel length.

So, in order to change the degree of anisotropy, one of the three variables in equation 2.1 should be changed. In previous literature these options were explored, so the next sub-section will give an overview. Additionally, some anisotropy ratios will be calculated from the available data.

2.3.1 Printing Temperature

The printing temperature has an effect on the anisotropy of the structure. This includes both the bed temperature and the nozzle temperature. The way that the temperature affects this is through sintering. Sintering is defined as the coalescence of particles under the action of surface tension, and it takes place above the glass transition temperature T_g of the filament being extruded [11]. In essence, a more efficient sintering process causes better bonding between traxels, and thus a lower contact resistivity σ in each direction [12]. It is also shown in previous research that heating the sample after printing reduces its anisotropy [13]. However, the printing temperature does not necessarily have an effect on the anisotropy as mentioned in [14].

2.3.2 Geometry

Another variable in equation 2.1 is the traxel width. In the y-direction this is the actual width of the traxel, and in the z-direction it is the height. From the equation, it should be the case that a wider traxel leads to a higher anisotropy ratio in the y-direction. The same goes for the height and the anisotropy ratio in the z-direction. Zhang et al [15] investigated the effects of changing the traxel size on the resistivity in both the vertical and horizontal directions. The results are shown in figure 2.2, where A, B, and C are defined as in figure 2.3.

In all samples, the resistivity in the z-direction was higher than in the y-direction. This would make sense, seeing as there is more contact between directly adjacent traxels. The left figure of figure 2.2 shows the resistivity in the vertical direction as a result of changing the geometry. It is clear that the greatest effect was made by changing the traxel width, so B. Increasing the width would increase the contact between vertically adjacent traxels, making the apparent resistivity lower. In the horizontal direction, however, the traxel height seemed to have the greatest effect. In this case, the anisotropy changes by removing material, which would be difficult to achieve in the context of this paper.

2.3.3 Infill Density

Infill density significantly influences the electrical anisotropy of 3D printed objects. A higher density causes larger contact in both the y and z-directions, decreasing the effective contact resistivity [16]. On the other hand, lower infill densities can create discontinuities and gaps in the conductive pathways, introducing greater anisotropy with varying electrical conductivity along each direction. Another factor to consider is that a lower infill density will make the object

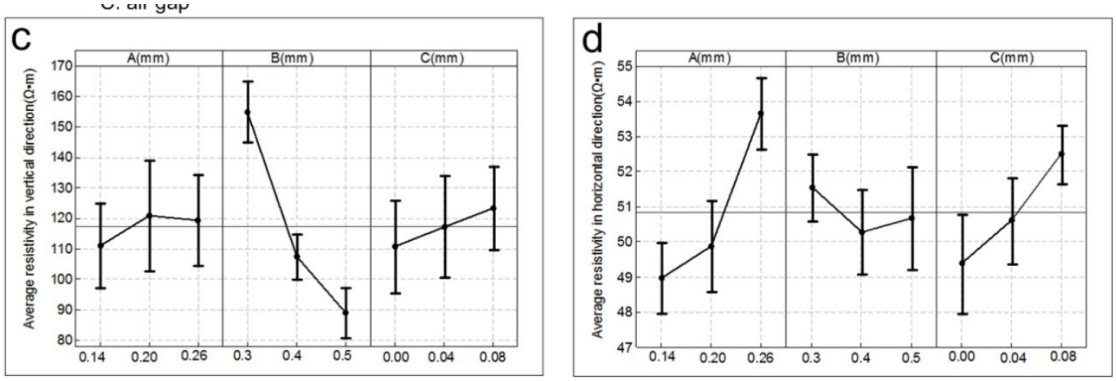

Figure 2.2: The Effect of Layer Thickness on the Resistivity of the Samples [15]

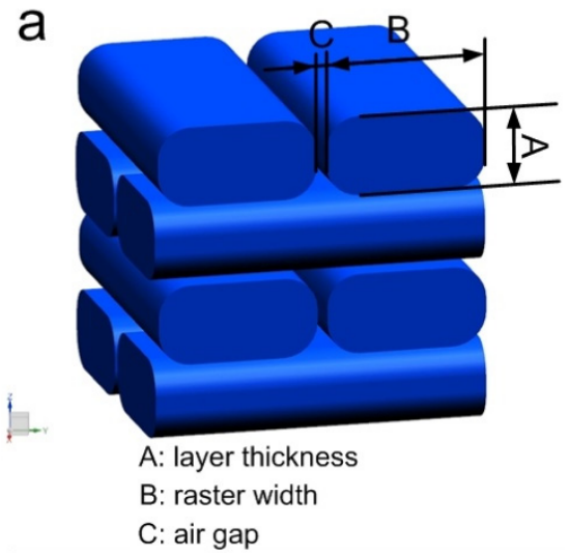

Figure 2.3: The Definitions of A, B, and C as described above [15]

less structurally sound. Making it so that larger gaps in between the traxels in the horizontal direction would lead to a higher apparent resistivity within each layer [15]. Due to the structural limitations, however, it could be difficult to implement in practice.

2.4 Anisotropy Ratios from Literature

Previous research has been performed on the resistivity and other electrical properties of 3D-printed samples. This section aims to use that literature to find the anisotropy ratio's of those samples. In this way, comparisons can later be made to the findings in this paper. Specifically Matic Arh [17] made some measurements on piezoresistivity on 3D printed conductive samples under mechanical stress. Before putting the samples under stress, initial measurements were made, which is relevant for this paper. The homogenized resistivity values were given for each direction, and are presented in table 2.1. The ratio x/y gives Γ_y and the ratio x/z gives Γ_z, as shown in equations 2.3 and 2.4.

Direction	Initial Resistivity (Ω cm)
x	20.96
y	32.96
z	33.83

Table 2.1: The Homogenized resistivities in each direction [17]

$$\frac{x}{y} = \frac{20.96}{32.96} = 0.6359 = \Gamma_y \tag{2.3}$$

$$\frac{x}{z} = \frac{20.96}{33.83} = 0.6196 = \Gamma_z \tag{2.4}$$

2.5 Conclusions

In order to change the anisotropy in 3D-printed samples, the printing temperature, geometry, or infill density can be varied. The printing temperature can be varied within the workable range of the material. As for the geometry, the height of the layers of traxels could be adjusted. Changing the infill density is less relevant for this paper, as the investigation is about the anisotropy in the material itself, not the air gaps. Values for the anisotropy ratios from literature were also calculated.

3 The Model

This section will give an overview of the derivation of the model, starting from the 2D case and showing how it evolved into the full 3D model. The full derivation for these two models was shown in [8] and [7] respectively, and will therefore not be discussed in detail. It should be emphasised that this section is based entirely on the work of Dijkshoorn et al. and Daniel Wilmes.

3.1 2D Case

The model was originally created for a 2D sheet, meaning that there are adjacent traxels, but only in a single plane [8]. The traxels have electrical properties on their own longitudinal axes as well as on the contact planes between adjacent ones. These can be described by partial differential equations like the following [7]:

$$\frac{\partial \hat{U}_2(x,\omega)}{\partial x^2} + \frac{\Gamma(\omega)}{W^2}\left(2\hat{U}_2 - \hat{U}_1 - \hat{U}_3\right) = 0 \tag{3.1}$$

3.1.1 Anisotropy Ratio Γ

In equation 3.1 dimensionless number Γ is introduced. This number represents the ratio of the bulk properties and the contact properties, and will henceforth be referred to as the anisotropy ratio. The derivation is shown in [8], but the result is as such:

$$\Gamma = \frac{\left(\frac{\rho}{1+j\omega\rho\epsilon_0\epsilon_r}\right)}{\left(\frac{\rho}{1+j\omega\rho\epsilon_0\epsilon_r}\right) + \left(\frac{\frac{\sigma}{W}}{1+j\omega\sigma C_0}\right)} \tag{3.2}$$

Note that for DC ($\omega = 0$) this expression is identical to the on given in Chapter 2.

3.2 The 3D Model

From the 2D model, a 3D model was created by D. Wilmes [7]. In this case, there are bulk and contact properties in both the y and the z-directions, and thus separate anisotropy ratios for those directions. Figure 3.1 shows how the traxels are numbered, from left to right, starting again once the end is reached. For the 2D case, only the bottom plane applies.

For this research, the focus will also be on the DC case, so the imaginary parts of the impedance and any capacitance can be ignored. In the y-direction, the number is effectively the same as in the 2D-case. As such:

$$\Gamma_y = \frac{\rho}{\rho + \sigma_y / W} \tag{3.3}$$

In the z-direction, the conditions are the same as in the y-direction, except the dimensionless number is then:

$$\Gamma_z = \frac{\rho}{\rho + \sigma_z / H} \tag{3.4}$$

3.2.1 The New Equation

Implementing equations 2.1 and 2.2 into equation 3.1 results in a new equation for the 3D model. This reads as follows:

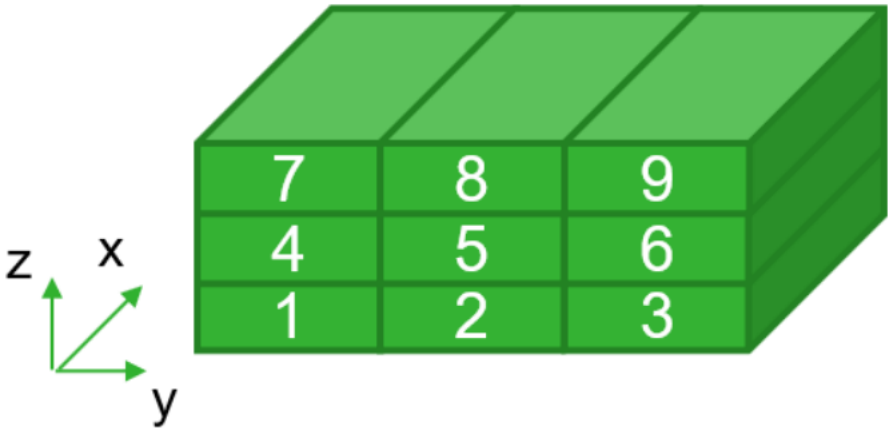

Figure 3.1: An Example of a 3-by-3 cube, demonstrating how the traxels are numbered [7]

$$\begin{aligned} &\lambda^2 \hat{U}_5(x,\omega) \\ &+\frac{\Gamma_y(\omega)}{W^2}\left(2\hat{U}_5(x,\omega)-\hat{U}_4(x,\omega)-\hat{U}_6(x,\omega)\right) \\ &+\frac{\Gamma_z(\omega)}{H^2}\left(2\hat{U}_5(x,\omega)-\hat{U}_2(x,\omega)-\hat{U}_8(x,\omega)\right)=0 \end{aligned} \tag{3.5}$$

All relevant properties and variables are defined in table 3.1.

Parameter	Label	Unit
Width per traxel	W	mm
Length	L	mm
Number of traxels	N	-
Volume resistivity	ρ	Ωm
Surface Resistivity y	σ_y	$\Omega\,\mathrm{m}^2$
Surface Resistivity z	σ_z	$\Omega\,\mathrm{m}^2$
Longitudinal Capacitance	ϵ	$\mathrm{F\,m}^{-1}$
Surface Capacitance y	C_y	$\mathrm{F\,m}^{-2}$
Surface Capacitance z	C_z	$\mathrm{F\,m}^{-2}$
Anisotropy Ratio y	Γ_y	-
Anisotropy Ratio z	Γ_z	-
Voltage in traxel n at location x	$\hat{U}_n(x,\omega)$	V

Table 3.1: Definition of Model Parameters

3.3 MATLAB Implementation

This section shows the results of the model being implemented in MATLAB. A highly anisotropic sample is shown to illustrate the capabilities of the model. In addition to the voltage distribution, the model also displays current density and power over the surface of the sample. Figure 3.2 shows these graphics.

3.4 Conclusions

The model can be used to generate representations of the voltage distribution over samples, according to the parameters provided by the user. This representation can be both graphical

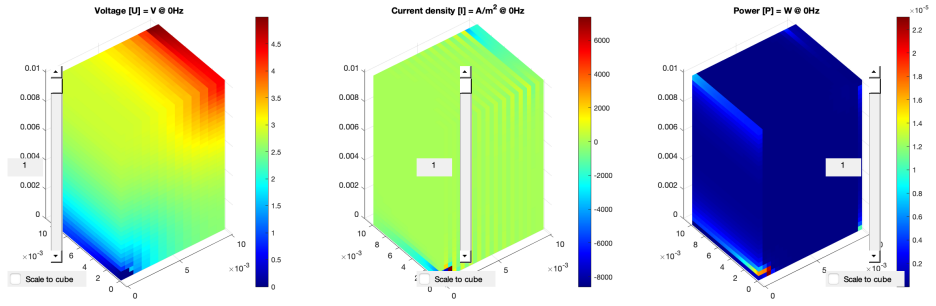

Figure 3.2: An example of the model output, displaying voltage, power, and current distributions

and numerical. The goal of the model in this paper is to use it to predict the results to be obtained experimentally. From that prediction, the anisotropy can be found. It is with this information that an inference can be made as to whether the model accurately represents real samples. An example of an anisotropic model output is also shown.

4 Design and Fabrication

This chapter aims to answer the research question: **How can a set-up be designed that is capable of producing data that is comparable to the model?** As such, it describes the fabrication process of the samples and the set-up needed to test them.

As described in chapter 3, the model produces graphical and numerical representations of the voltage distributions over samples. The goal of the set-up should subsequently be to measure the voltage distributions over the real samples. This would allow for comparison between the expectations from the model and the obtained results. Knowledge from chapter 2 can also be used to produce samples with different expected anisotropies. The sections below give an overview of the fabrication of these samples and the setups to perform the various measurements.

4.1 The Sample Design

This section describes the design process of the samples, the choices made in which parameters to vary, and the method in which electrical contact was established with the samples.

4.1.1 3D-printing

The samples are created through the process of 3D-printing. This process has a few main steps. First, a 3D-model is created using CAD software. For this paper, SolidWorks was used. That model is then exported to a slicing software. This software shows how the model can be printed, according to parameters set by the user. PrusaSlicer was used for the samples in this paper. Lastly, the slicer software generates G-code, which are the instructions for printing that can be sent to the printer.

4.1.2 The Structure of the Samples

The exact shape and structure of the samples had to conform to a few criteria. Firstly, the sample had to be in the shape of a cube, which was easily achieved by simply making a cube in the CAD software. The cube form was chosen so that all measured sides would have the sam dimensions, making comparison much easier. This initial cube is shown in figure 4.1. The cube designed was 10 mm wide, high, and deep. Further dimensions and printing parameters are given in chapter 5.

The next step was to design connection points for the electrical contacts. The contact and ground points have to be on opposite corners, making contact with the first and last traxel respectively. The initial design idea was to have simple extrusions with a width and height of exactly one traxel. A clamp could then be used on each of these extrusions to provide the contacts. This design proved too flimsy to function well, so the extrusions were made thicker, to be exact. This thickness of the extrusions was maintained regardless of the layer thickness of the sample. This ensured that the samples were capable of being compared to each other. This version of the design is shown in figure 4.2.

The design was polished as experiments were performed, specifically to improve the electrical contacts and reduce the effects of contact resistance. This is elaborated upon in the next section. The final design included "towers" on the extrusions, and holes in which the contact wires could be melted. The gap to the towers was small enough that it could be bridged by the 3D-printer. This final version is shown in figure 4.3.

The samples were printed in batches of 3. The printed samples are shown in figure 4.4.

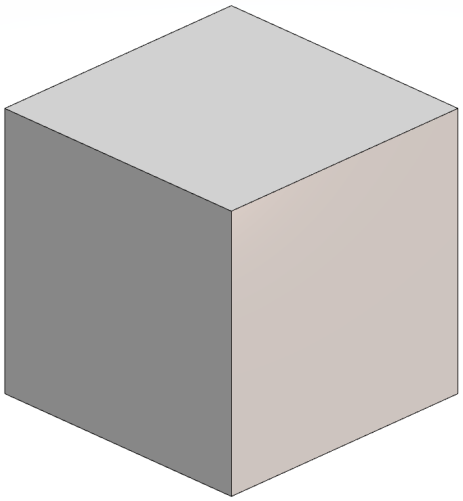

Figure 4.1: The Block

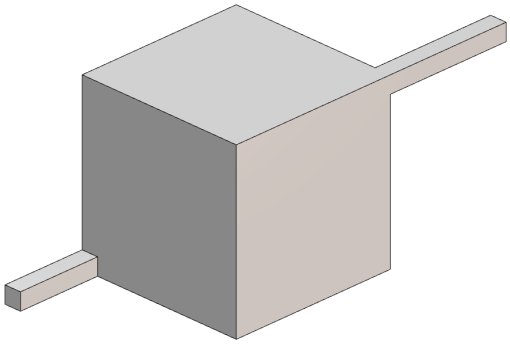

Figure 4.2: The Block with Extrusions

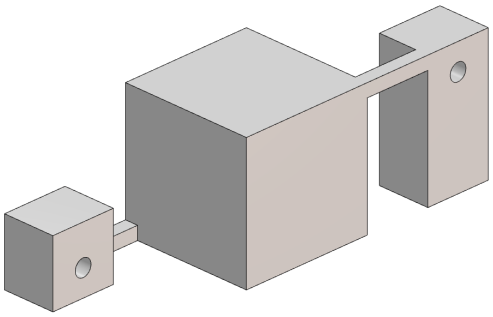

Figure 4.3: CAD Model of the Final Design

4.2 The Electrical Contacts

A challenge in designing the cubes and the rest of the setup was ensuring that the electrical contacts between the sample and the wires were adequate. This was achieved through multiple avenues.

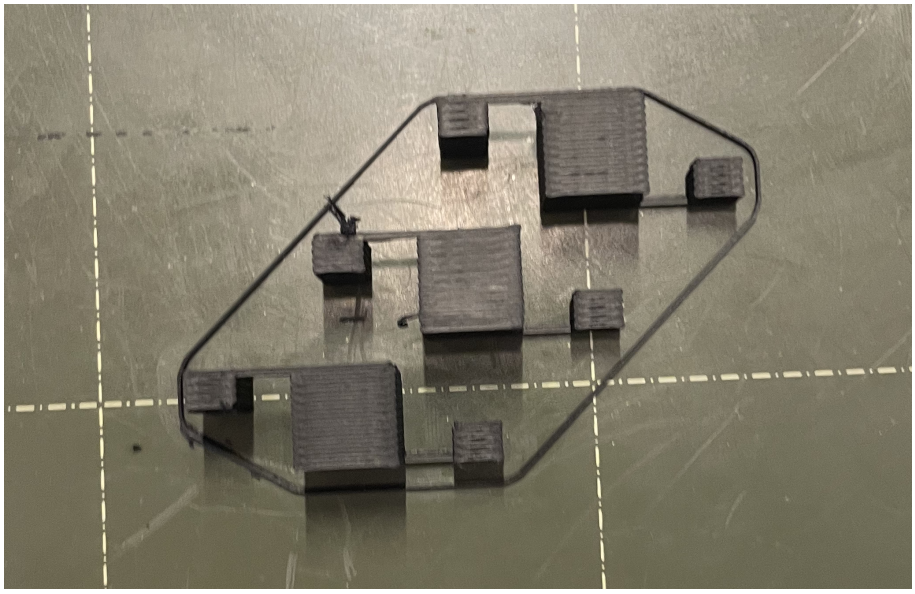

Figure 4.4: The Printed Samples

4.2.1 Melting the Wire into the Sample

The first method that was used was melting the wire into the sample. The exposed part of the wire was inserted into the holes as shown in figure 4.3. The holes were then melted shut around the wires, which ensured that the wire could not wiggle, and thus affect the contact with the sample The limited movement ensured that the amount and force of the contact would remain relatively constant throughout the experiments.

4.2.2 Silver Paint

The second method used towards improving the contact was using conductive silver paint. The towers and the extrusions were covered in silver paint, creating what was in practice a metal plating around the structures. This paint also made contact with the exposed parts of the wire, causing them to have the same voltage as the one that would be imposed by the source.

4.3 An Overview of the Samples

In total, five different samples were printed and tested, each with their own unique parameters. The printing temperature and the layer thicknesses were varied.

4.3.1 Printing Temperature

Two different printing temperatures were tested, 195°C and 225°C. These were decided upon due to the properties of the material used in printing, Protopasta. According to the documentation these are the outer limits of which the material is capable of being printed. Going too cold would risk jamming the extruder, and also not produce a proper product. Printing too hot would cause the material to exit the nozzle in an uncontrolled manner, and cause stringing on the product. It could even burn the material, which would produce additional unwanted effects.

4.3.2 Layer Thickness

The samples were printed and tested with three different layer thicknesses. These were: 0.1 mm, 0.2 mm, and 0.3 mm. As mentioned in chapter 2, the variation of these thicknesses should affect the resistivity of the traxels and change the anisotropy of the samples. Achiev-

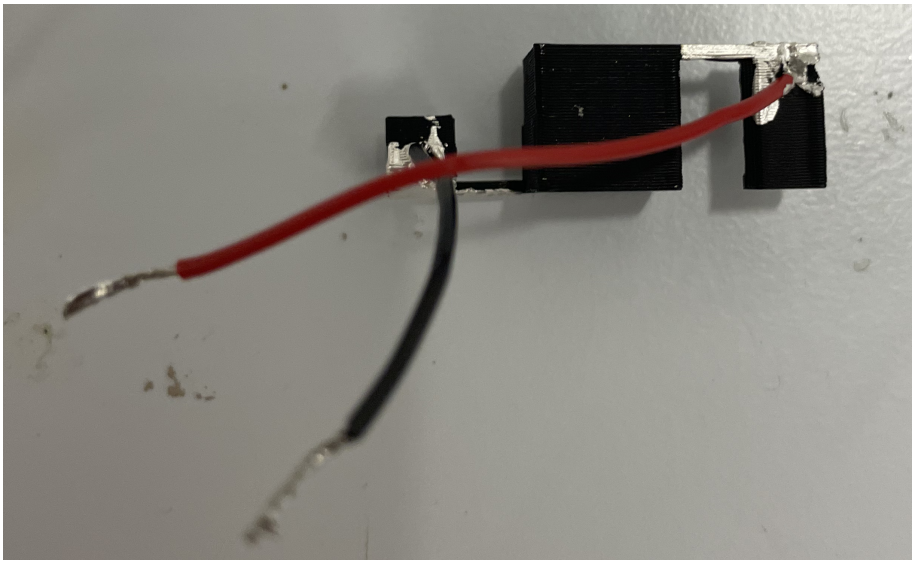

Figure 4.5: A Sample with the Silver Paint and Melted Contact Points

ing these different thicknesses was simply done by changing the layer thickness setting in the PrusaSlicer program.

4.3.3 Printing Parameter Overview

Table 4.1 gives an overview of the samples to be printed. Samples 1 and 2 are printed with the same layer thickness and a different temperature. For samples 3, 4 and 5 the layer thickness was varied but the printing temperature kept the same.

Parameter	Sample 1	Sample 2	Sample 3	Sample 4	Sample 5
Layer Thickness	0.2 mm	0.2 mm	0.1 mm	0.2 mm	0.3 mm
Nozzle Temperature	195 °C	225 °C	210 °C	210 °C	210 °C
Bed Temperature	60 °C	60 °C	60 °C	60 °C	60 °C

Table 4.1: The Printing Parameters and Geometric Properties for each Sample

4.4 Setup Design

The voltage over the surfaces of the cube was measured using a pogo pin with a rolling tip. This was based on the work of M. Schouten [18]. This pogo pin was attached to a modified 3D printer called the Flexionstein. The Flexionstein was originally a Rova3D printer on which a Duet 2 was mounted to use as a control board.

In order for this method to be functional, three additional tools were needed. One was a script that would generate the G-Code required for the purposes of the experiment. G-code is the programming language used to control 3D printers. A script with certain commands for the path, speed, and extrusion speed is fed to the printer, which subsequently executes those commands. The second was a holder for the sample, so that it would stay in place during the measurements. Lastly, a holder was designed for the pogo pin that could be easily mounted on the Flexionstein.

4.4.1 Sample Holder

To ensure that measurements were stable and repeatable, a holder was designed to keep the sample in place during experimentation. The design required three main features: a way to secure the holder to the platform, slits for the extrusions of the sample to go through, and a

way to hold the sample in place securely. Figure 4.6 below shows the CAD model of the final design. The slits below the extrusions of the holder allow for the extrusions of the sample to be accessible. The distance between the beams was given some leeway with respect to the width of the samples. The holes allow for a nut and a bolt to tighten the clamp's grip on the sample. In this way, no movement is possible. the flaps on the side of the sample holder allow for the component to be secured on the platform with duct tape. Figure 4.7 shows the printed sample holder mounted on the platform.

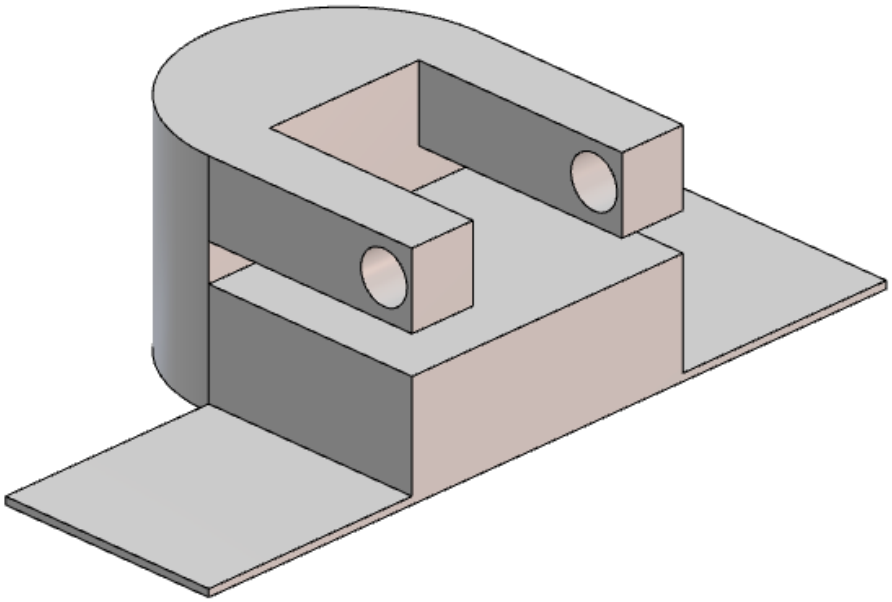

Figure 4.6: CAD Model of the Sample Holder

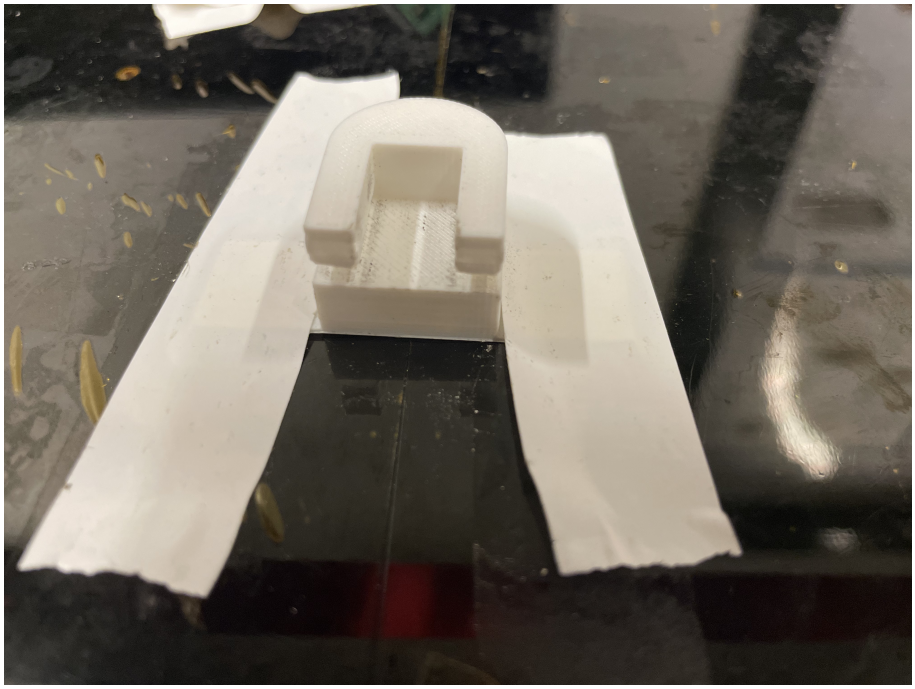

Figure 4.7: The Mounted Sample Holder

4.4.2 Probe Holder

The second necessity for the setup was the probe holder. This component needed to be able to hold the rolling pin in place whilst rolling over the sample. It also needed to be capable of being mounted on the Flexionstein. Figure 4.8 shows the holes on either side of the object. These allowed for the component to be mounted on the printer using nuts and bolts. The square hole in the center allows for the probe to go through it from the top, with a wire connected to it. Figure 4.9 shows the bottom view of the CAD model, with a small hole for the probe. This hole was precisely dimensioned to ensure that the probe was securely fastened during measurements, but could also be easily removed in case of any issues. The probe holder was 3D printed with white tough PLA, and mounted on the Flexionstein printer as shown in figure 4.10.

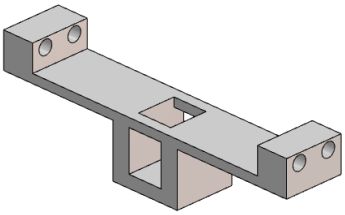

Figure 4.8: CAD Model of the Probe Holder

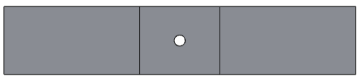

Figure 4.9: Bottom of the Probe Holder

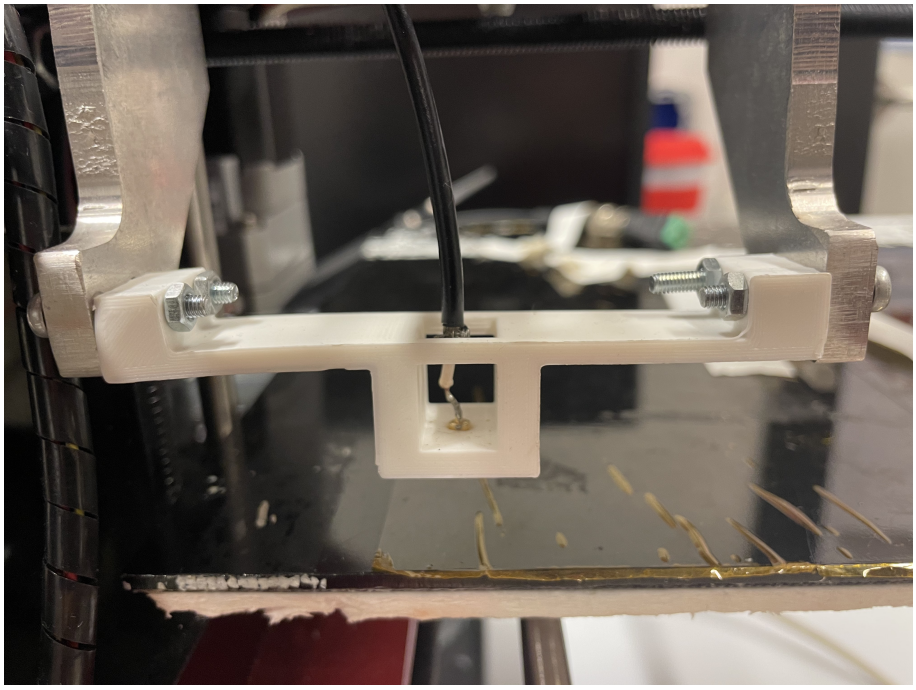

Figure 4.10: The Probe Holder Mounted on the Flexionstein

4.4.3 Generating G-code

In order for measurements to take place, the adapted 3D printer had to be controlled effectively, having the printer head with the probe meander over the surface of the cube. As mentioned, 3D printers are controlled by G-code. Hand-writing this code was an option, but it was more efficient to create a G-code generating program.

The program for the generation of the G-code was written in MATLAB. The script had to be adaptable and easily re-calibrated in case changes in the setup were made throughout exper-

imentation. These conditions were well-met. The user of the code can easily implement the starting position of the printer head, as well as the step sizes for each meander. The speed of the probe is also easily adjusted in the initial conditions. The program causes the printer-head to move a defined distance in the x-direction, from the starting point. It then takes a step in the y-direction, the magnitude of which is also defined by the user, after which it returns to the starting x-coordinate. The code generates this pattern for a user-defined number of iterations, creating a meander pattern.

4.5 Conclusion

This chapter gave an overview of the fabrication of the samples, the method of electrical contact with those samples, and the design of the overall setup. An explanation was also given for additional necessities such as the G-code generating program.

5 Methodology

This section describes the methodology for the execution of the experiments, as well as the methodology for the processing of the raw data.

Three experiments were performed, one of which was a sort of sub-experiment. Firstly, the voltage distribution across four faces of the samples was measured. This is the core experiment of the paper, which serves to find the anisotropy in the samples. As a sub-experiment to that, the bulk resistance of the samples were measured. This is a necessary parameter for the data analysis. Lastly, some additional experiments were performed to verify the precision of the method.

5.1 Measuring the Voltage Distribution Across the Faces of the Cube

The core experiment of this investigation is to measure the voltage distribution across the surface of the samples,

5.1.1 The Experimental set-up

Materials

The following list describes the items, programs, and any other necessities for the set-up.

- Flexionstein (Adapted Rova3D Printer)
- The samples
- Keithly DAQ6510 (Data acquisition module)
- Power Supply E030-1 Delta Elektronika
- Sample Holder
- Probe Holder
- Omniball™ Spring loaded pin probe with roller head
- Coax cables
- Cable adapters
- Nuts and bolts
- USB drive
- G-code generating Program

Description and Photo

Figure 5.1 is a photo of the entire setup. This includes the power supply and DAQ on the left, and the adapted 3D-printer on the right. Coax cables were used to connect the DAQ to the probe, as well as the power supply to the sample. This was done to reduce interference from the various power loops in the setup.

5.1.2 Measurement Procedure

After completing the set-up, the first step is to insert the first desired sample into the holder. If this is the first experiment, the next step is to calibrate the G-code generator to the starting point. Manually guide the probe to the bottom-left corner of the sample. The coordinates

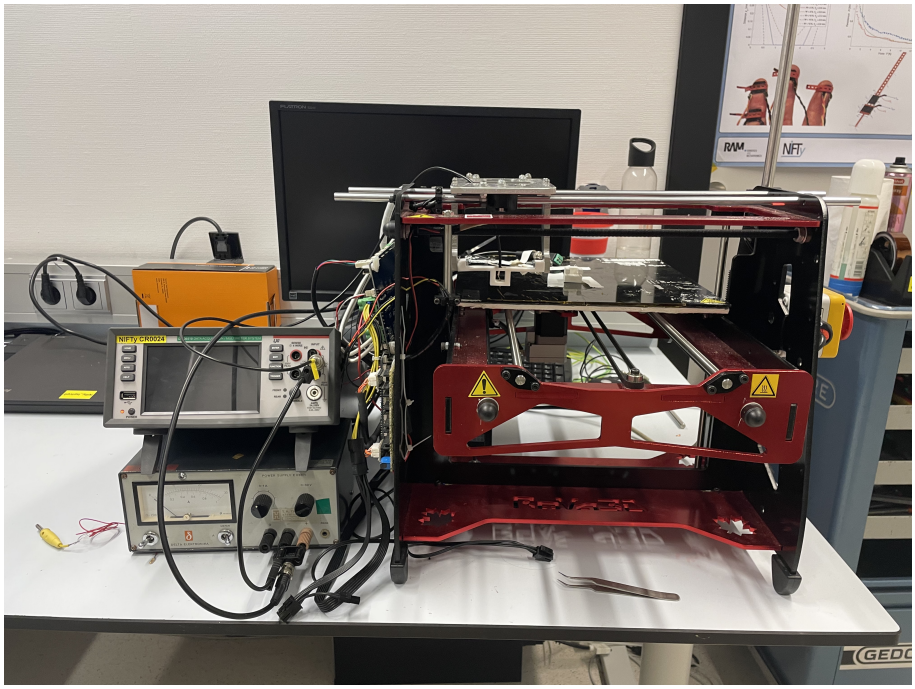

Figure 5.1: The Complete Setup

shown on the user interface can then be inserted into the program, which, after running, will produce the full G-code for the experiment. This can then be transferred to the Flexionstein interface. If the sample holder is not moved, this can be used for all subsequent samples.

The fabricated samples should all have wires connected to them. Insert these into the corresponding terminals from the coax cable, and fasten the screws on the adapter. Turn on the power supply and the data acquisition modules. Ensure the sample and the probe are secured in their holders, and that the buffer on the DAQ has been cleared. When ready, start the measurement with the G-code file in the interface. Watch the graph to ensure measurements are up to your expectations. Once the measurement is finished, go to the log section of the DAQ, and tap "Save to USB". The data is then transferred to the drive. Disconnect the sample from the power supply, and turn it 90 degrees to the next side to be measured. Repeat the measurements for each side, and then repeat this entire process for the desired amount of samples.

5.1.3 Data Processing

The data obtained from this experiment must be processed so that it can be used to present a visual representation of the voltage distribution. The data obtained from the DAQ6510 is just the voltage and the time stamp. To turn this data into a voltage distribution, each voltage measurement must be linked to x, y-coordinates of the surface. Since the speed of the printer-head is known, the time-stamp can be used to determine the distance traveled by the probe. The dimensions of the sample then help determine the coordinates corresponding to that distance.

5.2 Measuring the Bulk Resistance of the Samples

Another experiment that was necessary for determining the anisotropy ratios of the samples was measuring the bulk resistance of the samples. For this experiment, a four-point measurement was used. This method is used in resistance measurements to negate issues with contact resistance.

5.2.1 Four-point Measurement

For a simple impedance measurement, a multi-meter with two probes could be used to measure the impedance between two points . However, this method includes the contact resistance between the probe and the measured component. For this reason, it was necessary to use a four-point measurement to find the impedance of the samples. The method uses 2 pairs of probes, one pair carrying a current and the other pair sensing voltage. Figure 5.2 shows the configuration of the probes, where the voltage is measured in between the two current carrying probes. In this way, there is an imposed current and the voltage is measured. Ohm's law is then used to calculate the impedance. This is all done automatically using data acquisition equipment. On the samples, the probes will be connected on the portions covered in silver paint. Important to note is that the measurement will then still include the contact resistance between the silver paint and the sample. This resistance is very small, however, so it is negligible compared to the total resistance.

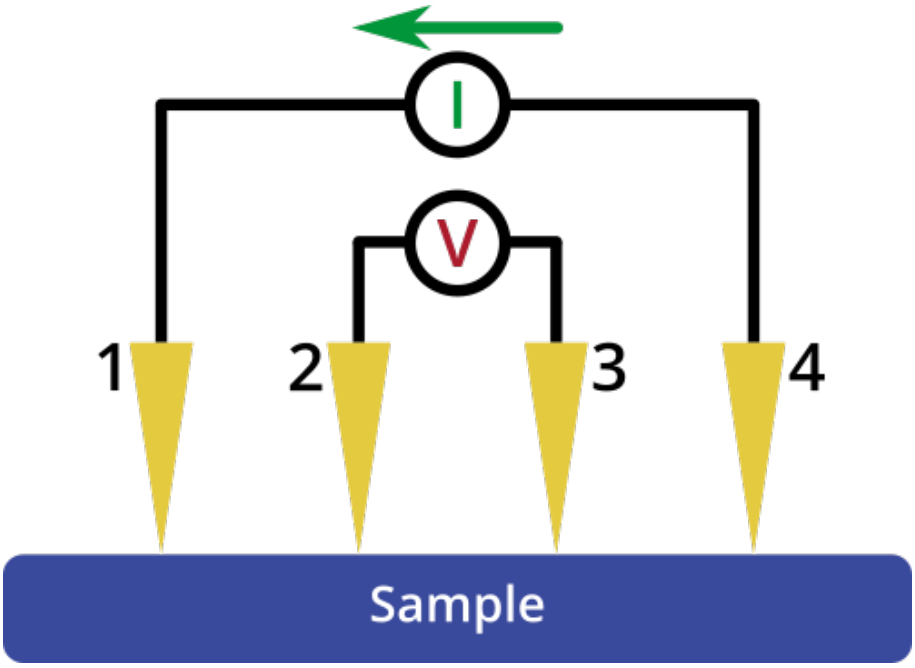

Figure 5.2: A diagram of the 4-point Measurement [19]

5.2.2 The Experimental set-up

Materials

- Keithley 2420 SourceMeter
- Samples
- 2 wires with crododile clips
- Wires to connect to sample
- Sample Holder

Description and Photo

Figure 5.3 shows the 4-point measurement being performed. For the current-carrying wires on the outside, the same cable was used as in experiment 5.1. For the voltage sensing wires, cables with crocodile clips were used. The sample holder was used to keep the sample stable, albeit in a slightly different manner than during the voltage measurement experiments.

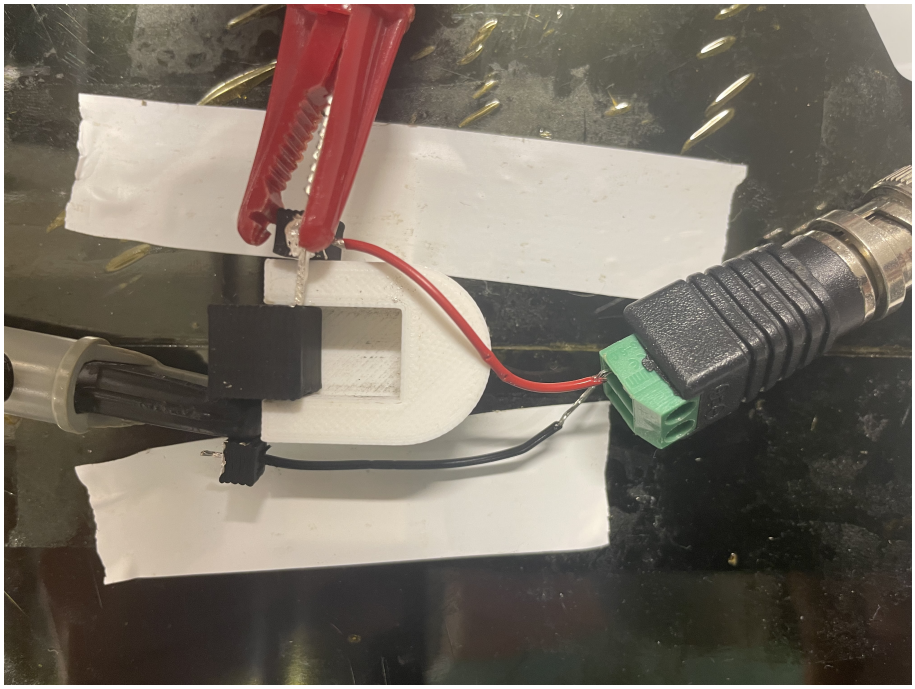

Figure 5.3: The setup for the 4-point Resistance Measurement

5.2.3 Measurement Procedure

The first step is to activate the right measurement program in the Keithly SourceMeter. This can be found in the ohm-sensing programs, with the 4-wire measurement being one of the options. Then, connect the wires already attached to the sample to the current output of the SourceMeter. Then, connect the wires with crocodile clips to the extrusions covered in silver paint. These should be connected to the voltage sensing terminals of the SourceMeter. Turn on the output of the SourceMeter, and read the resistance value off the interface.

5.2.4 Data Processing

The value for the bulk resistance of the samples is used to find ρ. This process is explained in the next section.

5.3 Fitting with the Model

With the collected data from the previous 2 experiments, the steps for the processing of the data can be undertaken. The goal of the processing is to turn the raw data of the voltage distribution into a color coded 2D diagram of each side, as well as a grand 3D image. This, together with the resistance values, can be used with the model to determine the anisotropy ratio's for each sample.

In order to fit the obtained data with the model, the anisotropy ratios must be recalled from chapter 3. These were as follows:

$$\Gamma_y = \frac{\rho}{\rho + \sigma_y / W} \tag{5.1}$$

$$\Gamma_z = \frac{\rho}{\rho + \sigma_z / H} \tag{5.2}$$

In each of these equations, there are three unknown variables. W and H for the y- and z-anisotropies respectively are known, as they are set during printing. ρ, Γ, and σ are the variables to be found. The first step is to find Γ in both directions. This is achieved through visually fitting

the outcome of the model with the experimental results. The values for Γ are adjusted until the potential distribution in the model conforms to the data. From there, the measured bulk resistance values are used to find ρ.

Since the values for Γ are now known, σ can be expressed as a function of ρ. These functions are shown in equations 5.3 and 5.4. The model must now be adjusted so that the bulk resistance value displayed for that simulation is equal to the one measured. Since ρ is a combination of the bulk resistivity and the two σ values, is proportional to the bulk resistance. Thus, the correct value of ρ can be found by changing its value until the correct bulk resistance value is shown. The σ values then follow implicitly.

$$\sigma_y = \left(\frac{\rho}{\Gamma_y} - \rho\right) * W \tag{5.3}$$

$$\sigma_z = \left(\frac{\rho}{\Gamma_z} - \rho\right) * H \tag{5.4}$$

Some examples of graphics from the model are shown in figures 5.4 and 5.5.

Figure 5.4 is an example of a relatively isotropic sample, with voltage peaks at the contact and ground points. The rest of the surface has almost a uniform voltage of around 2.5 V. In this case, Γ_y and Γ_z were both at 1, meaning the surface resistivities between the traxels were of negligible impact.

Figure 5.5 shows an extreme example of anisotropy, specifically in the z-direction. Γ_y is 1 in this case, and Γ_z 0.0033. This kind of anisotropy is not expected in the real samples, as the difference in resistivity in the two directions would have to be significantly large.

Through manual fitting of the model by adjusting the values of the two surface resistivities, a representation of the obtained measurements can be found. These will then produce values for the anisotropy ratio's.

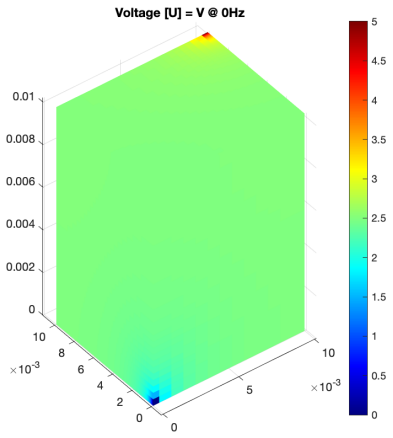

Figure 5.4: A 3D Graphic Generated from the Model displaying very Little Anisotropy

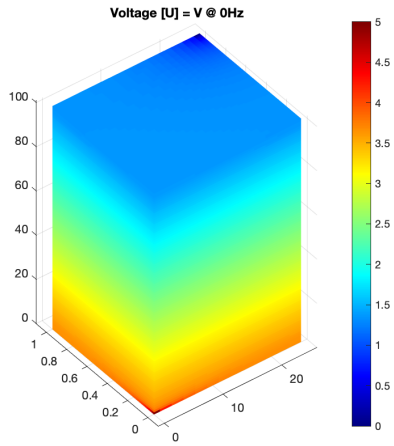

Figure 5.5: A 3D Graphic from the Model Displaying High Anisotropy in the z-direction

5.4 Verification of the Method

Some additional measurements were performed to verify that the measurements were consistent and precise. The goal is to determine whether repeating the same measurement with the same sample would yield the comparable results, i.e. if the measurements are reproducible. The experiment also verifies whether the direction of measurements makes a difference for the measured values. As such, the experiment consists of two parts. The first is to measure the

voltage distribution on the top side of the sample three times, with the probe moving along the traxels. The second is to do the same, but with the probe moving perpendicularly to the traxels.

5.4.1 The Experimental set-up

The set-up of the experiment is the same as when measuring the voltage across the faces of the cube. A sample was chosen arbitrarily, in this case one printed at 195 °C with a layer thickness of 0.3 mm.

The one change that is required to obtain data is for the measurement taken with the probe meandering perpendicularly to the traxels. The G-code generator must be adjusted to generate a meander in that direction. This is a case of switching the x- and y- coordinate generators, since the area to be measured upon is a square.

5.4.2 Measurement Procedure

As with the set-up, the procedure for this experiment is largely similar to the one in section 5.1. Calibrate the G-code generator to the starting position of the sample if necessary. Then, turn on the power source and the DAQ6510. Start the measurement and watch the graph to ensure measurements are qualitatively up to expectations. Once the measurement is finished, save the data to a USB drive. Repeat the measurement two more times, without adjusting the position of the sample.

5.5 Conclusion

There are three experiments to be performed. One is measuring the voltage distributions over the sides of the sample. This is performed with a probe attached to a modified 3D-printer rolling over the surfaces Another experiment is to measure the bulk resistance of the samples, for which a four-point measurement is used. Lastly, some measurements are made to verify the method.

6 Results

This chapter presents the results from the three experiments described in chapter 5. First, the results from the verification experiments are presented. Then, resistance values are shown. Subsequently, the measured voltage distributions for all samples are shown. Lastly, the results of the process of fitting the model to reality are shown. Every result presented is accompanied by a short analysis.

6.1 Verification

This section shows and describes the results of the experiments performed to verify the method. Measurements are performed along the traxels and perpendicularly to them. Figures 6.1 and 6.2 show a roung indication of the paths, for reference. Note that many more meanders were taken in actual measurements, and the traxels were not followed exactly.

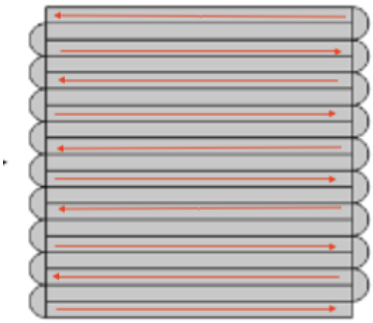

Figure 6.1: The rough measurement path along the traxels [6]

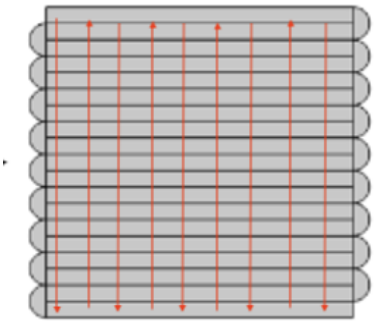

Figure 6.2: The rough measurement path perpendicular to the traxels [6]

Probe Moving Along the Traxels

Figure 6.3 shows the voltage distribution of the top side of a sample, measured three times. The probe rolled along the traxels. Visually, the voltage distribution looks almost identical in all three measurements. This is further shown to be true in figure 6.4, where the raw data of the voltage distributions was plotted in the same figure. Except for some sudden troughs due to noise, the lines on the plot are almost identical. This indicates repeatability of the measurements.

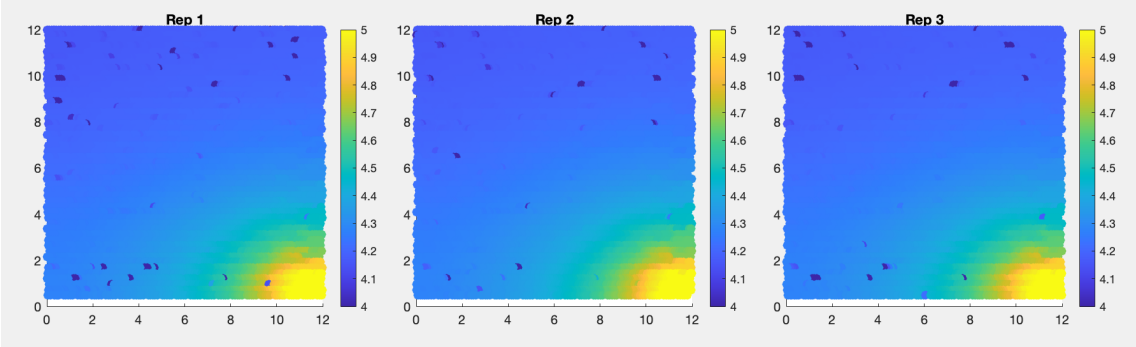

Figure 6.3: Three Repeated Measurements of the top of the Same Sample

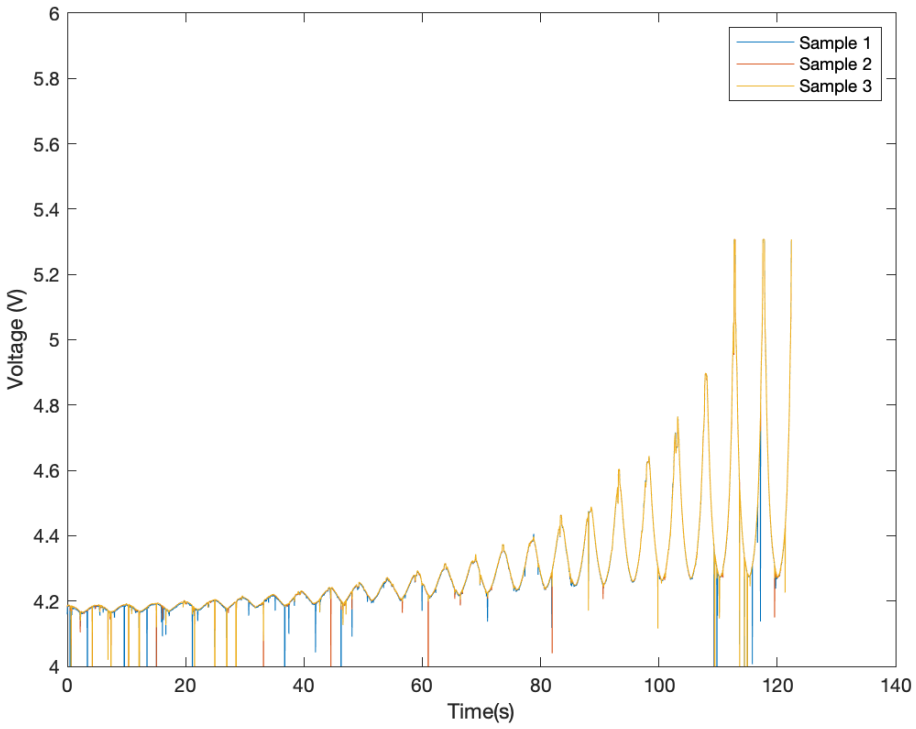

Figure 6.4: The Raw Data of the Voltage When Measured Along the Traxels

Probe Moving Perpendicularly to the Traxels

In figure 6.5, the measured voltage distributions are shown for when the probe meanders perpendicularly to the traxels. The first and second measurements look quite comparable, with the third measurement having a slightly lower voltage over the surface. This qualitative observation is supported by quantitative data in figure 6.6. The first two measurements follow a similar pattern, whereas the third starts similar but is then consistently lower throughout the measurement.

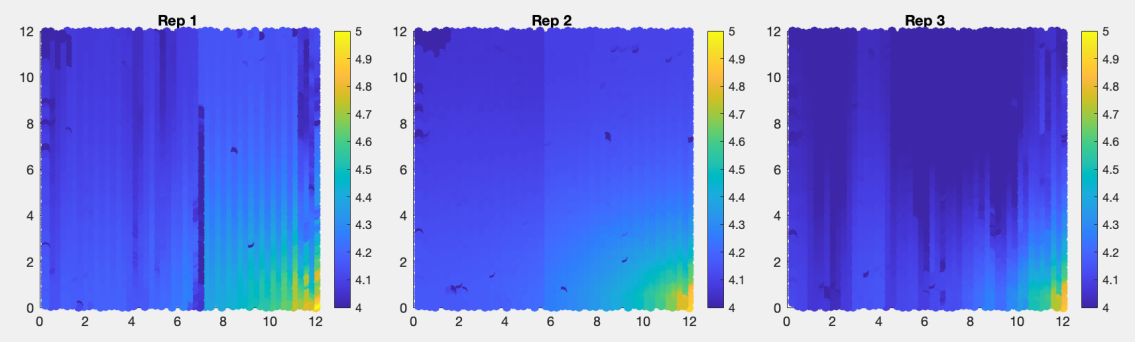

Figure 6.5: The Voltage Distributions When Measured Perpendicularly to the Traxels

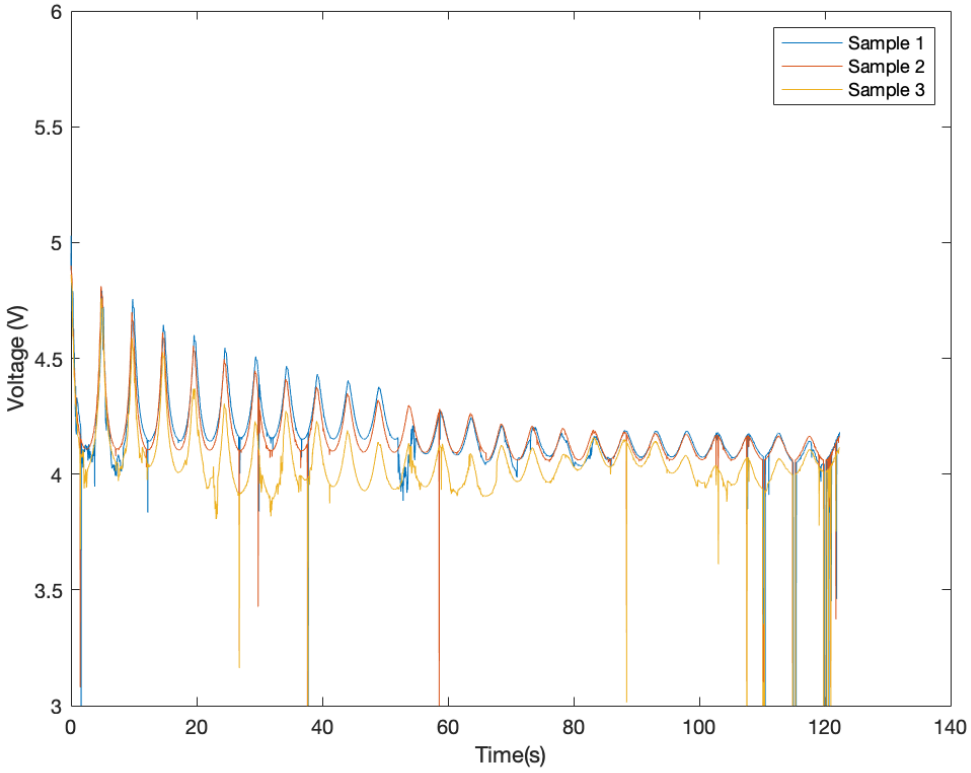

Figure 6.6: The Raw Data of the Voltage When Measured Perpendicularly to the Traxels

Comparison

Although the measurements were quite similar when measured in their respective directions, the measurements in different directions were quite different. Figure 6.7 shows the raw data from measurements in both directions. Important to note is that these measurements should not be equal, seeing as the voltages measured are not at the same positions. However, it is interesting to compare the height of the peaks, especially at the lowest and highest measured voltages.

Notable are the final peaks from the measurement along the traxels reaching around 5.3 V. On the other hand, the final peak of the perpendicularly measured sample reaches only 4.9 V. There are also multiple peaks in the former reaching that high voltage. This is likely due to the probe hitting a layer of silver paint on the edge of the sample. The orientation of the measurement could have caused this layer not to be hit during the latter measurement.

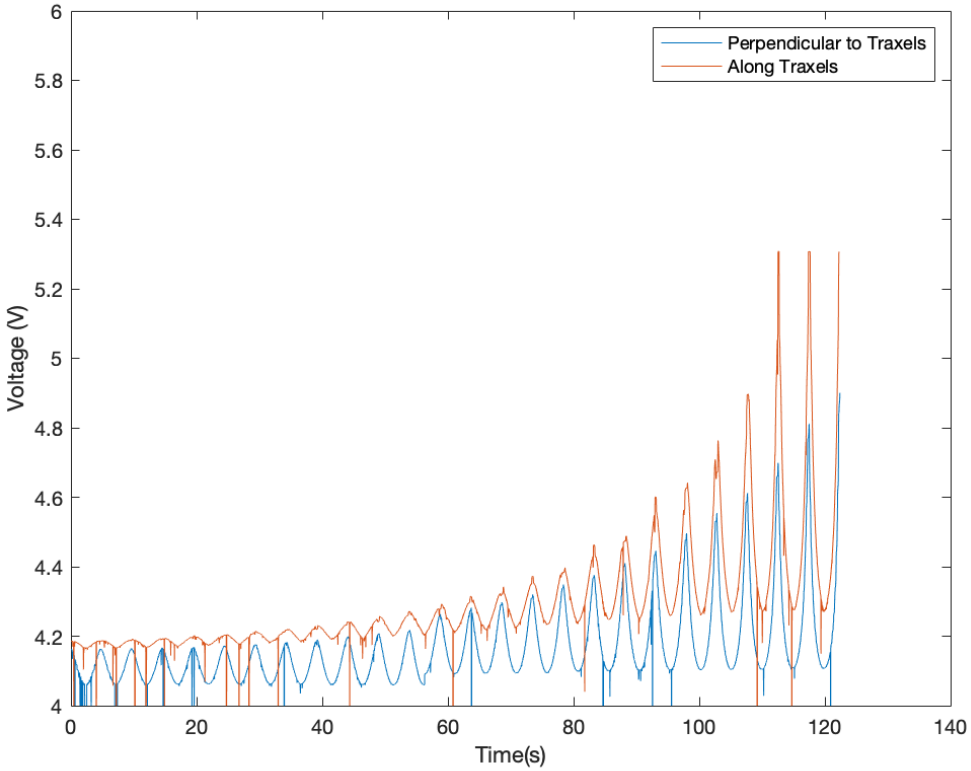

Figure 6.7: The raw data of two measurements, one measured along the traxels, and one perpendicularly to them

6.2 Resistance Values

Table 6.1 contains the results of the 4-point measurements that were performed to find the bulk resistance of each sample. Three samples were tested for each differing parameter. From the results, there seems to be a clear distinction in resistance when the printing temperature is varied.

6.3 The Voltage Distributions

The next few sections show the voltage distributions for all the measured samples. The top and bottom are indicated with their eponymous labels. Side V indicates the side on which the contact voltage was connected, and side G indicates the side on which the ground was

Sample	Resistance (kΩ)
1	0.221
2	0.465
3	0.332
4	0.312
5	0.383

Table 6.1: The Measured Bulk Resistance of each Sample

connected. The placement of the top and side V plots is such that the bottom and top of the plots connect on the sample. The same goes for the plots of the bottom and side v distribution. The sides are placed in such a way so that it is easier to read how well the sides connect to each other.

6.3.1 Raw Data

Figure 6.8 is an example of the raw data of the voltage measurements. Figure 6.9 also shows the data as separate images. The expectation for this data is that there would be peaks and troughs as the probe meandered over the sample, with the magnitude of the peaks increasing as the probe got closer to the source or the ground terminal. The peaks and troughs of traxels further away from the ground terminal have only a small variation of around 0.1 V. This was true for all samples and directions, which may suggest that the samples are mostly isotropic.

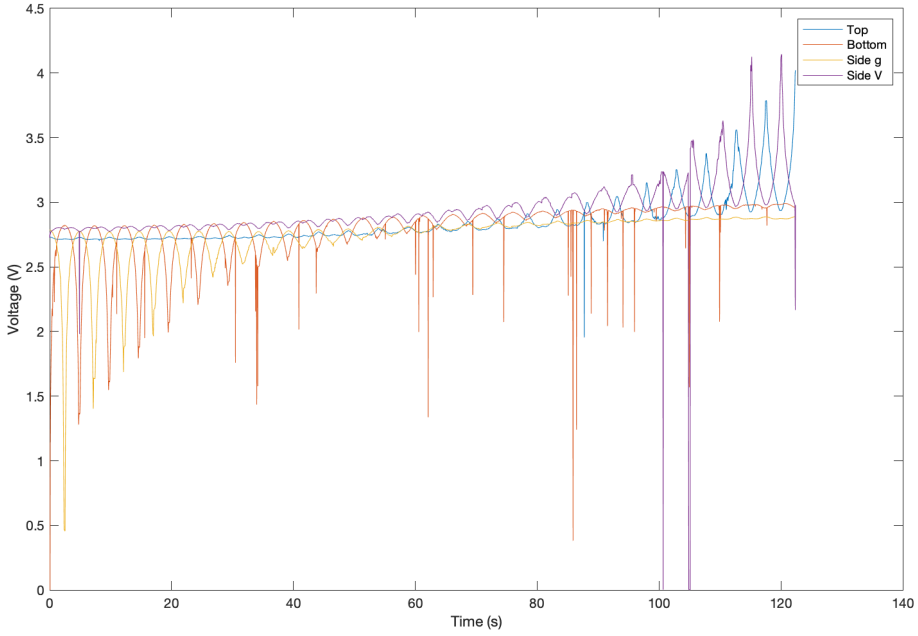

Figure 6.8: A Combined Plot of the four Measured Sides of a Sample.

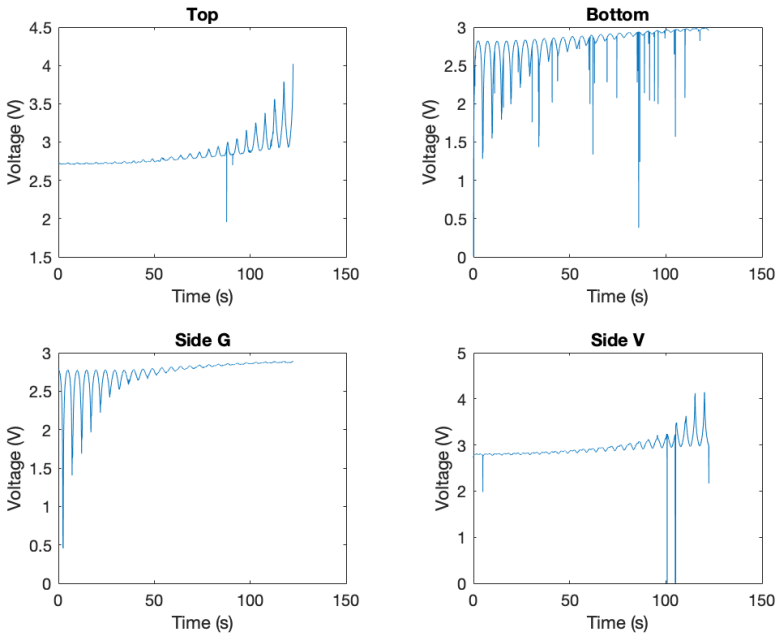

Figure 6.9: The Separated Raw Voltage of the Four Measured Sides of a Sample.

6.3.2 Printing Temperature

Figures 6.10 and 6.11 show the voltage distributions over the measured sides of the samples with a printing temperature of 195 °C and 225 °C respectively.

Sample 1 (195 °C)

Figure 6.10 shows the voltage distributions for the cube printed at 195 °C. Important to note for this sample is that the range was adjusted from 0 - 5 V to 0 - 2 V. This was due to issues with contact resistance. The bottom and ground sides clearly show the point of ground contact. The top side shows an input voltage of 2 V, but this value is not reached on the Side V plot. Due to these inconsistencies in the measurements, it could be difficult to make an approximation of the anisotropy.

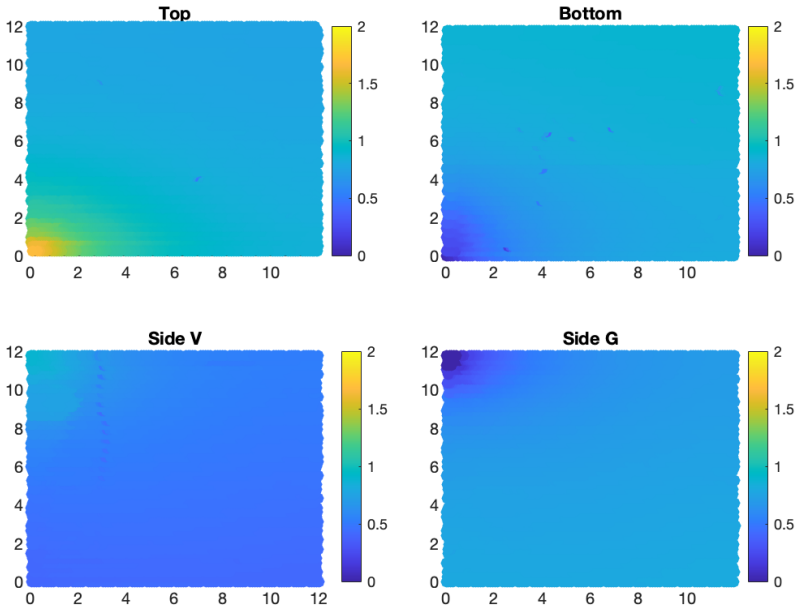

Figure 6.10: The Voltage Distributions for the 195 °C Sample(0V-2V)

Sample 2 (225 °C)

In figure 6.11, the voltage distribution for the sample printed at 225 °C is shown. The points of contact only affect a small corner of each side, after which the whole sample seems to be at around 2.5 V. This would suggest an isotropic sample. Something else of note is the increased noise on the bottom side of the cube, and, to a lesser extent, side G. The dark blue specks indicate a possible loss of contact. This could be the result of inconsistencies in the sample surface due to the high printing temperature.

6.3.3 Layer Thickness

Figures 6.12, 6.13, and 6.14 show a visual representation of the voltage distributions over samples printed with different layer thicknesses. These samples were all printed at a temperature of 210 °C.

Sample 3 (0.1 mm)

Figure 6.12 shows the voltage distribution over the four measured sides of the sample with a layer thickness of 0.1 mm. An initial observation that can be made is that the sample seems

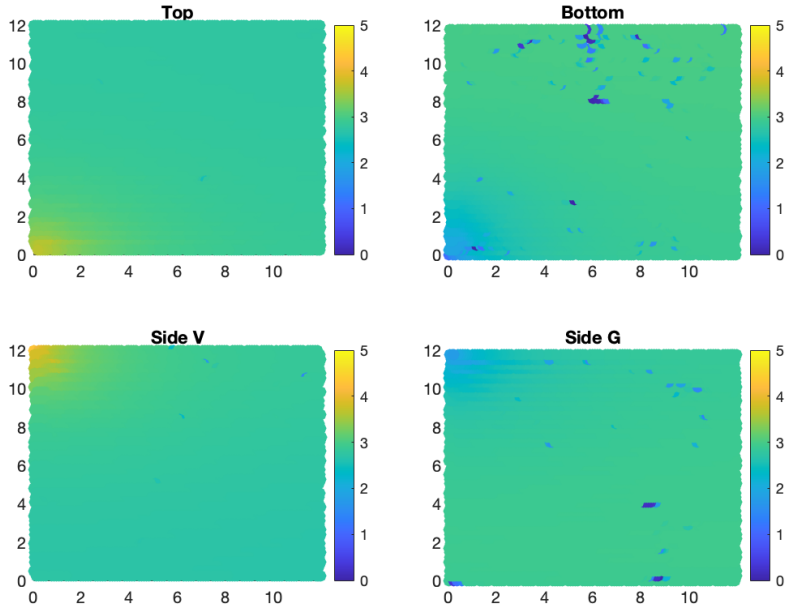

Figure 6.11: The Voltage Distributions for the 225 °C Sample (0V-5V)

quite isotropic. The contact points in the corners are clearly visible, with the voltage reaching the imposed 5 V and 0 V on either side of the spectrum.

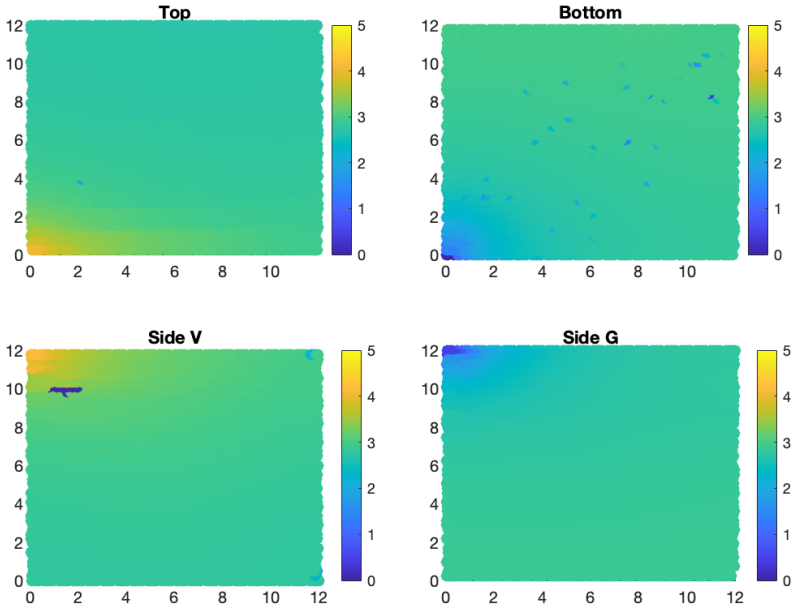

Figure 6.12: The Voltage Distributions for a 0.1 mm Sample (0V-5V)

Sample 4 (0.2 mm)

Figure 6.13 shows the voltage distribution over the four measured sides of the sample with a layer thickness of 0.2 mm. It can immediately be observed that the voltage at the ground contact point does not reach the imposed 0 V, but was measured at around 1.5 V. This indicates an issue with the contact resistance, where there was a large voltage drop between the contact point and the sample itself. The range of the colors were adjusted accordingly to more effectively demonstrate the voltage distributions.

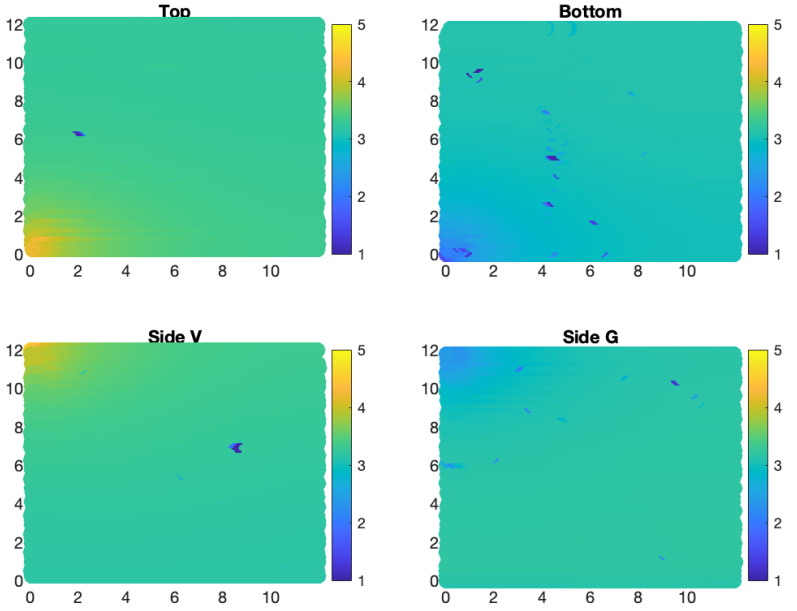

Figure 6.13: The Voltage Distributions for the 0.2mm Sample (0V-5V

Sample 5 (0.3 mm)

Figure 6.14 shows the voltage distribution over the four measured sides of the sample with a layer thickness of 0.3 mm. The most noticeable features of these plots are the dark blue lines in corners of all four sides. These lines are in places that would not be expected, as they are not at the ground terminal. The source of these discrepancies is likely the loss of contact of the probe with the sample. There also seems to be a difference in the shape of the distributions on each side. The top has a prominent section at the imposed 5 V, whereas the bottom only has the very bottom left corner at 0 V.

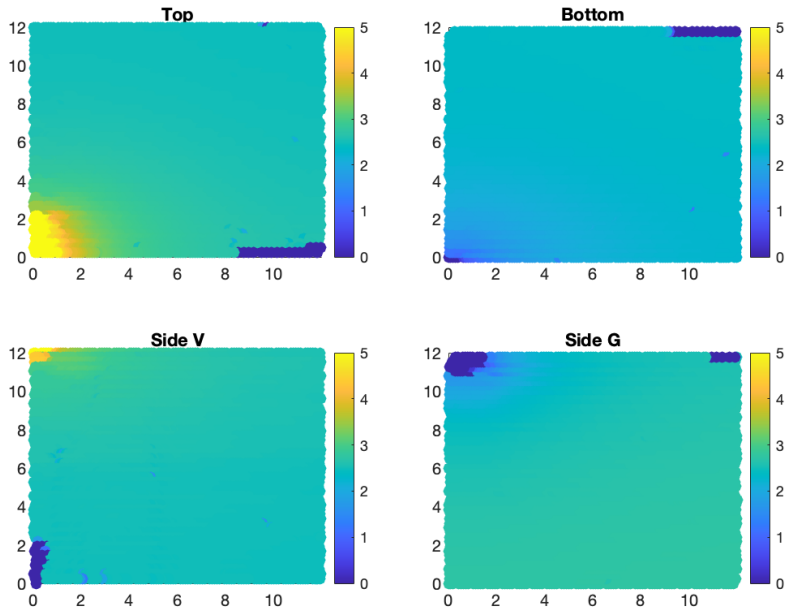

Figure 6.14: The Voltage Distributions for the 0.3mm Sample (0V-5V)

6.4 Fitting with the Model

This section shows the results of fitting the data with the model. The model is used to find the anisotropy ratios as described in chapter 5. A visual comparison of the voltage distribution from the model is compared to the one found experimentally. Table 6.2 shows an overview of the model parameters for each sample, and the resulting values for the anisotropy ratios in the y- and z- directions. The anisotropy ratios were all quite close to 1, meaning that samples were relatively isotropic. Notable is that the anisotropy seemed to reverse in the samples printed at different temperatures. There was a clear increase in ρ as the layer thickness increased.

Sample	T (°C)	W (mm)	H (mm)	σ_y (Ωm^2)	σ_z (Ωm^2)	ρ	Γ_y	Γ_z
1	195	0.4	0.2	1.87×10^{-7}	1.73×10^{-8}	0.00110	0.73	0.89
2	225	0.4	0.2	1.67×10^{-7}	3.55×10^{-7}	0.00475	0.92	0.73
3	210	0.4	0.1	4.34×10^{-8}	3.48×10^{-8}	0.00173	0.94	0.83
4	210	0.4	0.2	1.83×10^{-7}	9.97×10^{-8}	0.00306	0.87	0.86
5	210	0.4	0.3	2.38×10^{-7}	7.92×10^{-7}	0.05900	0.99	0.89

Table 6.2: The Model Parameters and Anisotropy Ratio's

6.5 Conclusion

This section presented and processed the results of the three experiments. The verification experiments showed consistent measurements when repeated in the same direction, but not when measured in different directions. The resistances were measured successfully using the four-point probe method. The results were fitted with the model, and values for Γ and σ obtained.

7 Discussion and Conclusion

This chapter is a discussion on the fabrication, methodology and the results presented in this report. A conclusion is also written, which summarizes the report and makes some conclusions on the research questions based on the results. Lastly, some recommendations are given for improvements to further research in this field.

7.1 Discussion

7.1.1 Electrical contacts

One recurring issue in the measurement process of the samples was the inconsistent contact resistance between the different samples. Various methods were attempted to reduce the impact of this issue, but a consistent solution was not found. The use of a silver paint coating on the outside of the samples did solve the issue of contact resistance between the contact wire and the extrusions of the sample. The melting of the wires into the holes of the samples also prevented the contact wires from wiggling. The issue, however, lay in the transition from the extrusions to the bulk of the sample.

A possible issue is that only the surface of the extrusions have the imposed voltage. The resistance of the silver coating and the extrusion itself could cause a voltage drop before the sample is properly reached. A thinner extrusion could solve this issue, with the voltage then being applied more directly to the sample. Applying some silver paint on top of the traxels themselves could also help to reduce the voltage drop. Some parts of the traxels near the contact points would then be directly imposed at 5 V or 0 V, preventing the drop.

In the end, this issue did not hinder the anisotropy ratios from being derived from the samples. These ratios depend on the potential distribution, not their magnitude. As a result, some of the voltage ranges for the samples were adjusted. However, fixing these issues would ensure greater homogeneity between the results of the various samples.

7.1.2 Measurement Consistency

Another point of discussion is the consistency of the measurements. The results in section 6.1 show that the measurements are repeatable, especially when measured in the same direction. However, the measurements taken with the probe moving perpendicularly to the traxels were significantly different from when the probe moved along the traxels. This was shown in the visual representations of the distributions, figures 6.4 and 6.5. A possible cause of this is that the geometry of the sample is slightly different in the alternate direction. This could mean that the probe did not measure along the whole sample when measurements were taken perpendicularly to the traxels

To improve this experiment, more measurements could be done on a larger variety of samples. This would give a more complete picture of how consistent the measurements are, also when measured in a different method.

7.1.3 Measuring the Remaining Two Sides

In order to get a more complete picture of the samples, it could be useful to have the capability of measuring all six sides of the cube. The current design of the experiment did not allow for this, as the extrusions prohibited the two of the sides from being measured. A more flexible design could help to solve this issue, but that will make achieving suitable contact with the sample more difficult.

7.1.4 The Model

A big uncertainty in the results is the way that the model was used to approximate the anisotropy values of the measured samples. The visual appearance of the measured samples was used to fit the anisotropy ratio's, and this is prone to error.

The results show that most of the samples were very isotropic. The anisotropy ratios of all samples are close to 1 in both directions. When the values are that high, the differences in voltage distribution are minimal with slight variations in Γ This makes it difficult to conclude whether the determined values are correct. A possible improvement to the method is to use actual voltage values at points from the data, and fit them to those in the model. This could improve the accuracy of the values, as the factor of human error is eliminated. However, the isotropy of the samples would still make it difficult to determine any differences.

7.2 Conclusion

The conclusion aims to answer the research questions posed in chapter 1. Each question is addressed separately, and conclusions are made based on the results obtained in this paper.

7.2.1 The Fabrication of a Suitable Set-up

How can a set-up be designed that is capable of producing data that is comparable to the model?

The goal with this question was to create a set-up that was capable of measuring the voltage distribution over surfaces of 3D-printed samples. The data obtained should then have been able to be presented in a way that comparison and analysis with the model was possible. In some ways, this goal was achieved. There are also elements of the set-up that were unsuccessful, however.

The set-up of the modified 3D-printer, with a pogo pin capable of rolling over the surface of the sample, was a suitable one for measuring the voltage distributions. The data for each sample clearly shows the voltage on each measured side, with higher and lower voltages at the input and output points respectively. The roller pin was able to effectively measure the whole surface of each side, and produce results that ware comparable to the sides of the model. The adapted 3D printer (Flexionstein) also served its purpose well in this regard. The script written for it allowed the measurements to be calibrated for each sample and measure the sample in multiple directions. The probe holder held the probe stable and did not affect measurements. The sample holder held the samples in place effectively, preventing failed measurements.

There were also aspects of the set-up that could be improved, as mentioned in the discussion.

7.2.2 The Effect of Print Settings on Anisotropy

How do print settings such as nozzle temperature and layer thickness affect the anisotropy of the samples?

In general, most of the samples displayed a low amount of anisotropy. The voltages were higher and lower at the input and output terminals, but the rest of the sample had a mostly homogeneous voltage, usually the average of the input and output voltages. There were definite fluctuations in voltage throughout the samples as observed in the raw data plots, but only in a very small range. As a result, the anisotropy ratios were close to 1 in both directions for all samples.

Nevertheless, according to the fitting of the results with the model, there were differences in anisotropy between the samples. However, they did not seem to follow any pattern based on layer thickness or printing temperature. A higher printing temperature of 225 °C in sample 2 caused there to be more anisotropy in the $z-$ direction, whereas sample 1 printed at 195 °C had more anisotropy in the $y-$ direction. To improve the reliability of these findings, further

measurements should be made with a larger amount of temperatures. Also, multiple of the same samples should be tested. There is not enough data to reliably determine a pattern.

7.2.3 The Use of the Model to Approximate Anisotropy

To what extent can the model be used to approximate the anisotropy of real printed samples?

In the current configuration of the experiment, the validation of the model by approximation of the anisotropy is not reliable. The results obtained did not always display uniform anisotropy throughout the sample, and most samples displayed very little anisotropy in the first place. Due to the model displaying idealized versions of the samples, it was difficult to represent the measured data exactly in the model. The approximations were mostly based on the degree to which the input and output voltages propagated over the surfaces. The reason why the samples were so isotropic could be due to the printing process. In 2D, only one layer is printed, so the sample cools down relatively homogeneously. For 3D samples, however, multiple layers are printed on top of each other, reheating the layers below it.

7.3 Final Remarks

In general, much research can still be performed in the context of this experiment. More measurements can be taken on more samples, and a larger variety of parameters changed. Based on the results of this paper the anisotropic behaviour of 3D samples is much less defined than in the 2D samples, but the scope of the experiments were narrow compared to the possibilities. The model did allow for the anisotropy ratios and other parameters to be approximated through visual fitting. However, a different method such as fitting the numerical data to the model could yield more reliable results.

Bibliography

[1] N. Zohdi and R. C. Yang, "Material anisotropy in additively manufactured polymers and polymer composites: A review," *Polymers*, vol. 13, no. 19, 2021.

[2] S. J. Leigh, R. J. Bradley, C. P. Purssell, D. R. Billson, and D. A. Hutchins, "A simple, low-cost conductive composite material for 3d printing of electronic sensors," *PLoS ONE*, vol. 7, no. 11, 2012.

[3] M. Schouten, G. Wolterink, A. Dijkshoorn, D. Kosmas, S. Stramigioli, and G. Krijnen, "A review of extrusion-based 3d printing for the fabrication of electro- and biomechanical sensors," *IEEE Sensors Journal*, vol. 21, no. 11, pp. 12900–12912, 2021.

[4] A. Dijkshoorn, T. Hamstra, R. Sanders, S. Stramigioli, and G. Krijnen, "Dc electric metamaterial behaviour in tuned fused deposition modelling prints," in *2021 IEEE Sensors*, pp. 1–4, 2021.

[5] G. A. Folkertsma, W. Straatman, N. Nijenhuis, C. H. Venner, and S. Stramigioli, "Robird: A robotic bird of prey," *IEEE Robotics Automation Magazine*, vol. 24, no. 3, pp. 22–29, 2017.

[6] A. Dijkshoorn, M. Schouten, G. Wolterink, R. Sanders, S. Stramigioli, and G. Krijnen, "Characterizing the electrical properties of anisotropic, 3d-printed conductive sheets for sensor applications," *IEEE Sensors Journal*, vol. 20, no. 23, pp. 14218–14227, 2020.

[7] D. Wilmes, "Modelling, characterization and visualization of anisotropic electri- cal behaviour in cuboids of fused-deposition-modelling 3d prints," 2021.

[8] A. Dijkshoorn, M. Schouten, S. Stramigioli, and G. Krijnen, "Modelling of anisotropic electrical conduction in layered structures 3d-printed with fused deposition modelling," *Sensors*, vol. 21, no. 11, 2021.

[9] H. Surmen, F. Ortes, and Y. Z. Arslan, *Fundamentals of 3D Printing and Its Applications in Biomedical Engineering*, pp. 23–41. 07 2020.

[10] "Fused deposition modeling." https://nl.wikipedia.org/wiki/Fused_deposition_modeling/.

[11] S. Garzon-Hernandez, D. Garcia-Gonzalez, A. Jérusalem, and A. Arias, "Design of fdm 3d printed polymers: An experimental-modelling methodology for the prediction of mechanical properties," *Materials & Design*, vol. 188, p. 108414, 2020.

[12] C. Bellehumeur, L. Li, Q. Sun, and P. Gu, "Modeling of bond formation between polymer filaments in the fused deposition modeling process," *Journal of manufacturing processes*, vol. 6, no. 2, pp. 170–178, 2004.

[13] S. Stankevich, J. Sevcenko, O. Bulderberga, A. Dutovs, D. Erts, M. Piskunovs, V. Ivanovs, V. Ivanov, and A. Aniskevich, "Electrical resistivity of 3d-printed polymer elements," *Polymers*, vol. 15, no. 14, 2023.

[14] A. D. R. Fraser Daniel, Andy Gleadall, "Influence of interface in electrical properties of 3d printed structures," *Additive Manufacturing*, vol. 15, 2021.

[15] J. Zhang, B. Yang, F. Fu, F. You, X. Dong, and M. Dai, "Resistivity and its anisotropy characterization of 3d-printed acrylonitrile butadiene styrene copolymer (abs)/carbon black (cb) composites," *Applied Sciences*, vol. 7, no. 1, p. 20, 2017.

[16] T. Hamstra, "Realizing dc electric metamaterials through fused deposition modelling," 2021.

[17] M. B. Matic Arh, Janko Slavič, "Experimental identification of the dynamic piezoresistivity of fused-filament-fabricated structures," *Additive Manufacturing*, vol. 36, 2020.

[18] M. Schouten and G. Krijnen, "Characterization of 3d printed sheets using multi-frequency scanning impedance microscopy," in *2021 IEEE Sensors*, pp. 1–4, 2021.

[19] "4-point probe method." https://www.linseis.com/en/methods/4-point-probe-method/.